Characterization of a Pilot Fluidized Bed Reactor for Solar Calcination Processes

Thibaut Esence[1], Emmanuel Guillot[1], Michael Tessonneaud[1], Antoine Saraiva[1], Alex Le Gal[1], Mouâd Elidrissi[1], Damien Poncin[1], Jean-Louis Sans[1] and Gilles Flamant[1, a)]

[1] Processes, Materials and Solar Energy Laboratory, (PROMES-CNRS, UPR 8521), 7 Rue du Four Solaire, Odeillo, 66120, Font-Romeu, France

[a)] *Corresponding author: gilles.flamant@promes.cnrs.fr*

Abstract. Nowadays, the calcination of mineral particles is mainly performed by burning carbonaceous fuels. Consequently, this process is the second source of carbon dioxide emission worldwide. This study, developed in the framework of the SOLPART H2020 project, proposes a new concept of reactor-receiver for continuous calcination processes using concentrated solar energy. A pilot fluidized bed reactor has been designed and is currently under testing at the CNRS's 1MW solar furnace. The first experimental results show the feasibility of calcination processes with solar energy. A particle mass flow of around 20 kg/h of calcite has been decomposed into lime with a conversion rate around 20%. A numerical model has been developed and is still to be validated with more complete experimental data. A preliminary parametric study performed with the model shows that the conversion rate of the calcination process is strongly influenced by the mean residence time of the particles. Moreover, there is an optimal particle mass flow rate that maximizes the chemical efficiency of the system. This corresponds to a compromise between the reaction extent and the equilibrium temperature of the reactor.

INTRODUCTION

Calcination of minerals at high temperature (> 700°C) is widely used in various industrial sectors to produce chemical commodities (lime, cement clinker, phosphates, mineral oxides, etc.). After being crushed into powder, the minerals are usually treated at high temperature in rotary kilns or fluidized beds. Nowadays, the heat necessary to drive the endothermic calcination is mainly provided by the combustion of gas, coal or alternative carbonaceous fuels. Consequently, this process is the second source of carbon dioxide emission worldwide, behind power generation by combustion. Therefore, the use of renewable heat sources would allow reducing significantly the carbon balance of the concerned industries: cement and glass factories, metal industry, etc.

Three types of solar calcination reactors have been designed and tested. The cyclone enables processing continuously small particles (less than 10 µm [1-3] whereas a wide range of particle diameter (from 100 µm to some mm) can be treated in rotary kilns [4-7]. Contrarily, the fluidized beds can process about 50-500 µm particles with a narrow size distribution [5, 8]. The literature review indicates that only directly heated fluidized beds working in the batch mode have been reported.

This study investigates a new concept of solar reactor-receiver based on the fluidization technology for the processing of reactive particulates. The work was performed in the framework of the SOLPART H2020 project. The main proposed innovations are:

- compartmented fluidized bed,
- continuous operation,
- indirect heating of the particles and,
- solar power of about 50 kW.

Experimental tests have been performed to show the feasibility of continuous calcination processes with concentrated solar energy. First, the pilot fluidized-bed reactor is presented and the first experimental results are discussed. Then, a numerical modelling approach is described and a parametric study shows the main trends of the reactor behaviour depending on the particle mass flow rate and the fluidization flow rate.

EXPERIMENTAL WORK

Description of the Setup

A pilot-scale prototype of solar reactor-receiver has been tested at the 1MW CNRS's solar furnace (Odeillo, France). The setup manufactured by COMESSA (www.comessa.com) is a cavity-type solar receiver composed of a refractory cavity in which the reactor is located. The reactor (Fig. 1) is made of Nickel alloy 800HT (Nickel 32%, Chromium 20%) which can sustain temperatures up to 1100°C. It is 1-m long and has an internal width of 8 cm. It consists in four 25cm-long compartments in series in which the particles to treat are fluidized with air and heated at high temperature with solar energy to carry out the calcination reaction.

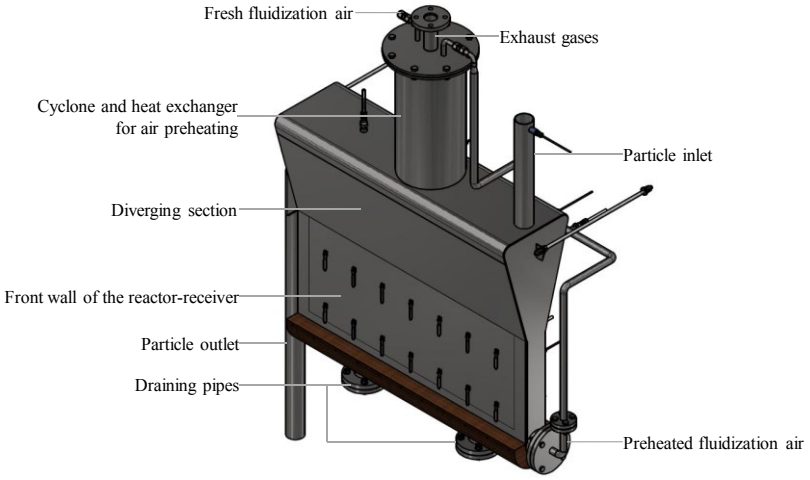

FIGURE 1. Pilot-scale reactor-receiver

A continuous flow of particles is treated (Fig. 2). The particles enter the reactor by gravity through a vibrating ramp. Since the particles in the reactor are fluidized, they behave like a fluid and overflow successively from a compartment to the other until the reactor's outlet. Then, they overflow towards an outlet storage tank or a sampling vessel. The separations of the compartments and the outlet of the reactor are designed so that the height of the fluidized bed is 40 cm. This corresponds to a fluidized-bed volume of 35 l, i.e. about 48 kg of particles (assuming a particle density of 2700 kg/m^3 and a fluidized bed void fraction of 0.5).

The fresh fluidization airflow passes through a preheating coil exchanger located at the top of the reactor and recovers a part of the heat of the extracted gases. The preheated air is then distributed at the reactor's bottom through a perforated tube, the fluidization distributor.

The hot fluidization air and the carbon dioxide produced by the reaction are extracted at the top of the reactor. They first pass through a diverging section which reduces the gas velocity and hence the amount of entrained particles. The gases then pass around the coil tube in which circulates the fresh fluidization air. As a result, the heat of the extracted gases is transferred to the cold fluidization air. Then, the gases pass through a cyclone to separate the gas and the remaining fine particles. While the fine particles fall back into the reactor, the gases are routed to a water-cooled exchanger and exhausted to the atmosphere through a bag filter.

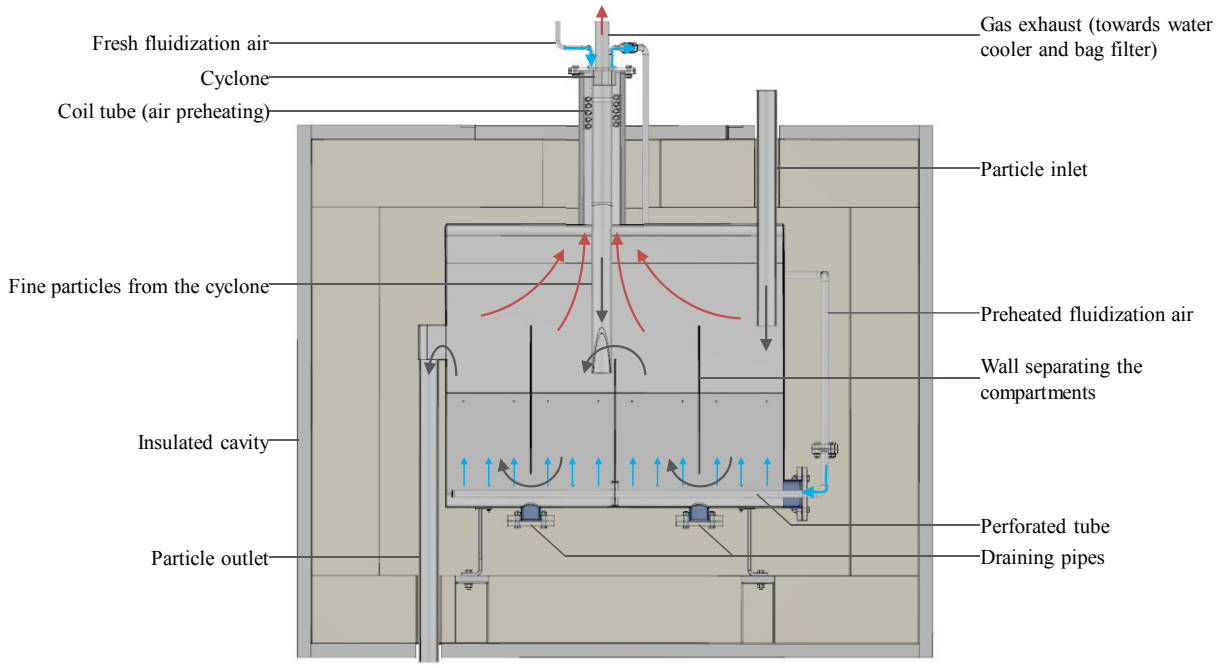

FIGURE 2. Cut-view of the reactor-receiver and the cavity with principle of particle and gas flows (─particles; ─fluidization air; ─exhaust gases)

During operation, the reactor's front wall is irradiated with concentrated solar flux (around 220 kW/m^2). The front wall is coated with the high temperature paint Pyromark® in order to improve its optical properties (increase the solar absorptivity). The flux absorbed by the front wall is transferred to the fluidized bed by conduction, convection and radiation. It provides the sensible heat and the reaction enthalpy required to perform the endothermic calcination reaction. The reactor is located in a solar cavity insulated with ceramic fibre. It reduces thermal losses caused by radiative and convective heat transfers to the outside environment. The front of the cavity is protected by a thermal shield made of aluminium and cooled by an internal water circuit. The aperture of the shield, which matches the aperture of the cavity (80 cm x 20 cm), may be closed by a shutter cooled with water as well. The shutter may be shift vertically to vary the size of the aperture and hence to control the solar power entering the cavity.

Instrumentation

The reactor and the cavity are equipped with 47 K-type thermocouples. There are 16 thermocouples welded on the front wall of the reactor-receiver. On the back and at the bottom of the reactor, 5 thermocouples are screwed on the wall and enable to calculate the energy balance of the reactor. Inside the fluidized-bed reactor, 20 thermocouples are located at various depth and width in each compartment in order to monitor finely the temperature of the fluidized bed. All these thermocouples enable to determine a representative average temperature of the bed, to characterize the thermal homogeneity of the reactor and to measure thermal gradients due to heat transfers in the fluidized bed. In addition, thermocouples are located at some key points of the loop: fluidization air before and after preheating, exhaust gas before and after the cooler, fines from the cyclone, particles in the cold storage etc.

Five pressure sensors are located at various heights in the reactor. An additional pressure sensor is located at the inlet of the air distributor in order to calculate the physical properties of the fluidization air.

The mass flow of fluidization air is measured by a thermal flow sensor Kobold KME (accuracy ± 3% of reading + ± 0.6 Nm^3/h). The mass flow and the physical properties (pressure and temperature) of fluidization air enable to calculate the average gas velocity in the reactor. The air mass flow is varied by using a needle valve in order to reach the set value. The mass flow of particles at the inlet of the reactor is controlled by a variator governing the vibration level of the vibrating ramp. During normal operation, it is not possible to measure directly the particle mass flow entering the reactor. That is why calibration tests were carried out in order to correlate the inlet mass flow rate of particles to the vibration level of the feeding ramp.

The reaction extent reached in the reactor during operation may be measured by two different ways. First, it is possible to measure the reaction extent by taking samples of particles at the reactor outlet. By weighting the samples before and after their complete calcination in an electrical furnace, it is possible to calculate the reaction extent of the samples with a mass balance. Second, a gas analyser measures the concentration of carbon dioxide in the exhaust gases of the reactor. By combining this value with the fluidization flow rate, it is possible to know the quantity of CO_2 emitted which is directly related with the reaction extent. In practice, this method is likely to be less accurate than the first one because the reactor is not sealed and some unknown air intakes from the atmosphere (e.g. through the particle inlet or outlet) may affect the CO_2 concentration in the reactor. However, contrary to the complete calcination of samples, this measurement is done in real-time. Therefore, it enables to monitor the reaction kinetics directly during the tests.

Tested Material

The first test campaign has been carried out with particles consisting of 93.8 m% of calcite ($CaCO_3$), the remaining part being non-reactive (CaO or impurities). The particle size distribution is given by Fig. 3. Since the density of calcite is 2710 kg/m^3, the particles used during the tests are classified as Geldart A-type particles [9]. The measured minimum superficial fluidization velocity of the particles is 3.8 mm/s at 20°C.

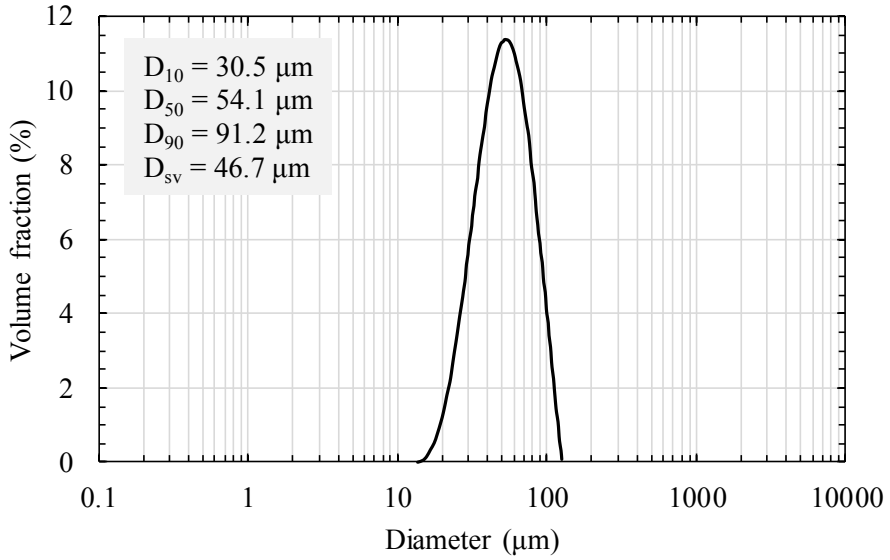

FIGURE 3. Size distribution of the calcite particles used during the first test campaign

Results and Discussion

A first calcination test has been carried out. This test was performed with a heliostat configuration leading to a solar concentration factor of 220 on the reactor's front wall. The average Direct Normal Irradiation (DNI) was 975 W/m² (decreasing from 1015 to 935 W/m² during the test). After 2 hours of heating, a quasi-steady regime was reached. During this particular period, the DNI was 950 W/m^2, the fluidization flow rate was 14.2 Nm^3/h, the preheated airflow temperature was 423°C, the shutter was covering 60% of the cavity aperture (upper part) and the vibration level of the ramp corresponded to an average inlet particle flow rate of 20 kg/h (according to the calibration tests).

Temperature Measurements

The stabilized thermal profiles are depicted in Fig. 4 and 5. In Fig. 4, the fluidized bed in all the compartments shows a relatively good thermal homogeneity. The average temperature is around 600°C, the maximum temperatures range from 650°C to 725°C and the minimum temperatures range from 450°C to 515°C. A maximum temperature of

858°C was reached in the second compartment at the very end of the test (after the stabilized period). Because of the use of the shutter to control the reactor's front wall temperature and avoid overheating, the thermal homogeneity of the front wall is not very good. Consequently, the heliostat aiming strategy will be refined for future tests.

Figure 5 shows that the temperature of the particles is quite homogeneous over the bed width. The average temperature difference between the front and the back of the fluidized bed is 150°C (except for the last compartment where it is 70°C). This shows the quality of the fluidization and the efficiency of the heat advection due to particle mixing.

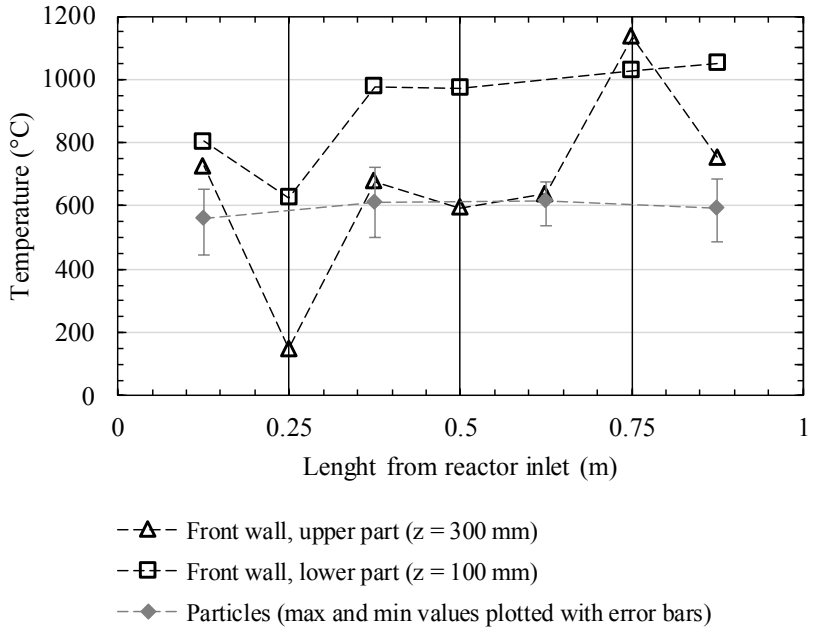

FIGURE 4. Temperature profiles during the first calcination test

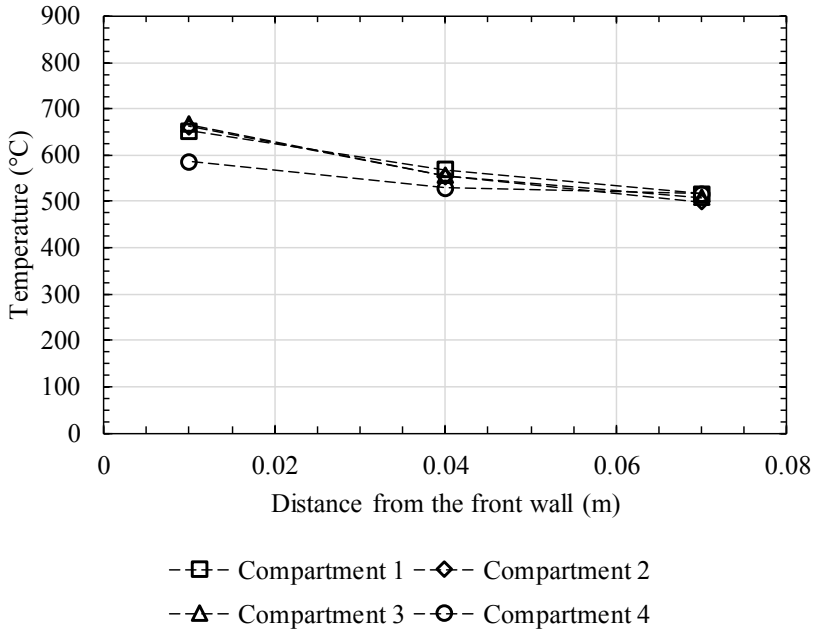

FIGURE 5. Transverse particle temperature profile in each compartment of the reactor at one third of the fluidized-bed height

Calcination Reaction and Mass Balance

The average outlet particle mass flow over the whole test was 7.2 kg/h, while the flow rate of entrained particles towards the filter was 5.0 kg/h (in spite of the internal cyclone). The reactor was emptied after the test and two samples corresponding respectively to the compartments 1 and 2, and 3 and 4 were taken. It was observed that a significant fraction of the bed in the reactor consisted of particle aggregates. Some of them were taken to be analysed.

All the samples were analysed by the complete calcination method: they were heated at 950°C during 3 hours in an electrical furnace. Assuming that all the calcite has been decomposed according to the reaction $CaCO_3 \rightarrow CaO + CO_2$, and no other reaction has taken place, the mass loss of the sample enables to calculate their conversion rate. The results are presented in Table 1.

TABLE 1. Results of the calcination measurements

Sample	Mass fraction of calcite (%)	Conversion rate (%)
Outlet storage tank	79.0*	15.8*
Filter	84.4	10.1
Compartments 1 & 2	78.1	16.8
Compartments 3 & 4	73.9	21.2
Aggregates	29.9	68.2

* Sample taken at the end of the quasi-steady state period

Table 1 shows that the conversion rate of the outlet particles was about 16% at the end of the stabilized period. The final conversion rates measured in the reactor after the test were respectively about 17% and 21% in the first and the second halves of the reactor. This difference between the outlet and the inside of the reactor may be due to several reasons: first, the reactor reached higher temperatures at the very end of the test (after taking the outlet sample); second, the aggregates of particles remained in the reactor. Table 1 shows that these aggregates exhibited a much higher conversion rate (68% in average).

In spite of the cyclone, a significant part of the particles (more than 40%) were entrained towards the bag filter, while the remaining part went to the outlet storage. Since the entrained particles were accumulated and mixed in the filter during the whole test, their conversion rate could have been significantly higher than 10% (Table 1) during the quasi-steady state period. Especially because the entrained particles are the finest ones, and hence the fastest to react.

It is also possible to estimate the conversion rate with the CO_2 concentration measured in the gas exhaust by the gas analyser. During the quasi-steady state period, the CO_2 concentration was 6.9%. Assuming that this concentration corresponds to the ratio between the molar flow rate of CO_2 produced by the reaction and the total molar flow rate of gas (air + CO_2), it is possible to estimate the mass flow rate of CO_2 produced by the calcination, and hence the flow rate of reacting particles. Following this procedure, the calculated mass flow rate of carbon dioxide produced during the quasi-steady state period is 2.1 kg/h and the corresponding conversion rate of calcite is 25%. This means that 2.6 kg/h of lime were produced during this period. Considering the uncertainties and the errors of measurement, such figures are consistent with the figures of Table 1 obtained with the complete calcination method.

Future Work

In order to increase the conversion rate of the particles, it is necessary to raise the average temperature of the fluidized bed. In the current configuration, the air preheating exchanger does not enable to raise enough the temperature of the fluidization airflow. As a results, the fluidized bed is cooled down by the airflow. To address this issue, an electrical air preheater will be implemented in order to preheat the temperature of the fluidization airflow as it will be done in an industrial solar reactor. In addition, the heliostat aiming strategy will be refined in order to increase the thermal homogeneity of the reactor's front wall and hence to increase its average temperature.

NUMERICAL MODELLING

A numerical model of the reactor has been developed to study the influence of the operation parameters on the performance of the system and to propose a scaling-up tool after validation. The numerical model coded with MATLAB aims to compute the wall and particle temperature, and the conversion rate of the calcination reaction in each compartment of the solar reactor at steady state. For that purpose, each compartment of the reactor is considered as an ideal stirred tank reactor. The conversion rate is computed from the reaction kinetics by using mass balances.

The temperatures of the front wall of the reactor (receiving the solar flux) and of the fluidized bed are computed by using energy balances. The reaction kinetics depends on the carbon dioxide concentration and the temperature. In addition, the heat transfer coefficient between the reactor's wall and the fluidized bed depends on the temperature and the particle properties. For this reason, it is necessary to use an iterative calculation procedure to solve the equations of the model.

Description of the Model

The temperature of the front wall of each reactor's compartment is defined by the energy balance (1) where φ_{abs} is the solar flux absorbed, φ_{IR} and φ_{conv} are the fluxes lost respectively by infra-red emission and convection, and $\varphi_{FB,F}$ is the flux transferred to the fluidized bed. As in the experimental tests, in the model, the concentration factor of the incident solar flux is limited so that the front wall temperature does not exceed 1100°C, the maximal temperature that the metallic reactor can sustain.

$$\varphi_{abs} = \varphi_{IR} + \varphi_{conv} + \varphi_{FB,F} \tag{1}$$

Then, the temperature of the fluidized bed is calculated according to the energy balance (2) where Φ_{in} and Φ_{out} are respectively the energies of the material flows entering (particles) and leaving (particles + carbon dioxide) the compartment, $\varphi_{FB,F}$ is the heat flux provided by the front wall (through the surface area S_F), $\varphi_{FB,B}$ is the heat flux lost through the insulated back wall (through the surface area S_B), Φ_r is the heat consumed by the endothermic calcination reaction, and Φ_{air} is the heat provided to the fluidization air.

$$\Phi_{in} + \varphi_{FB,F} \cdot S_F = \Phi_{out} + \Phi_r + \varphi_{FB,B} \cdot S_B + \Phi_{air} \tag{2}$$

In equations (1) and (2), the heat transfer coefficient between the walls and the fluidized bed is calculated with the empirical correlation of [10] in which the minimum fluidization velocity and the corresponding void fraction are calculated with the correlations from [11]. In addition, the radiative contribution is accounted for with a grey body approximation.

The heat consumed and the carbon dioxide produced by the reaction as well as the outlet particle mass flow rate and hence the mean particle residence time in each reactor's compartment depend on the average conversion rate α_{av}. To calculate this parameter, the reaction kinetics of calcite decomposition given by equation (3) is considered [12]. In this equation, t is the time, T the temperature, T_{eq} the temperature at equilibrium and P_{CO2} the partial pressure of carbon dioxide in bar. The CO_2 partial pressure at equilibrium $P_{CO2,eq}$ (in bar) is given by equation (4). Since each compartment is modelled as an ideal continuous stirred-tank reactor, the average conversion rate α_{av} is calculated according to equation (5) with τ_p the mean residence time of the particles [13].

$$\alpha(t) = 1 - \exp\left[-\left(5.55 \cdot 10^{-5} \cdot \exp\left(-\frac{337}{T - T_{eq}} \right) \cdot \left(P_{CO_2,eq} - P_{CO_2} \right) \cdot t \right)^2 \right] \tag{3}$$

$$P_{CO_2,eq} = 8.541 \cdot 10^7 \cdot \exp\left(-\frac{174970}{R \cdot T} \right) \tag{4}$$

$$\alpha_{av} = \int_{t=0}^{t=\infty} \alpha(t) \cdot \frac{1}{\tau_p} \cdot \exp\left(-\frac{t}{\tau_p} \right) \cdot dt \tag{5}$$

The mean residence time of the particles is calculated with equation (6) where ε is the void fraction of the fluidized bed calculated with the correlation (7) from [14], ρ_p is the average density of the particles, V_{FB} is the volume occupied by the fluidized bed in a compartment, and $F_{p,in}$ and $F_{p,out}$ are respectively the inlet and the outlet particle mass flow

rates. In equation (7), u_{air} and μ_{air} are respectively the superficial velocity and the viscosity of fluidization air, D_{sv} and Ψ_p are respectively the Sauter diameter and the sphericity of the particles, and g is the gravitational acceleration.

$$\tau_p = \frac{(1-\varepsilon)\cdot\rho_p\cdot V_{FB}}{\left(F_{p,in} + F_{p,out}\right)/2} \tag{6}$$

$$\varepsilon = \frac{1}{2.1}\cdot\left[0.4 + \left[4\cdot\left(\frac{u_{air}\cdot\mu_{air}}{D_{sv}{}^2\cdot\rho_p\cdot\Psi_p{}^2\cdot g}\right)^{0.43}\right]^{1/3}\right] \tag{7}$$

Parametric Study

The very first experimental results are not sufficient to firmly validate the numerical model. Additional experimental data to come are necessary. These data will be compared to the numerical results to confirm the relevancy of the model. However, at this stage, the developed numerical model describes the main interactions between the chemical and the physical phenomena occurring during the process. It is therefore possible to perform a parametric study to investigate the pattern of behaviour of the system depending on the operating conditions.

To analyse the results, two efficiencies are defined. The first one is the chemical efficiency (8) defined as the ratio between the heat actually consumed by the calcination and the incident concentrated solar power on the reactor front wall. The second one is the thermochemical efficiency (9) in which the heat provided to the materials (fluidization air, particles and CO_2) is assumed to be useful energy.

$$\eta_{ch} = \frac{\Phi_r}{\Phi_{solar}} \tag{8}$$

$$\eta_{thch} = \frac{\Phi_r + \Phi_{air} + \left(\Phi_{out} - \Phi_{in}\right)}{\Phi_{solar}} \tag{9}$$

Figure 6 depicts the influence of the inlet particle mass flow rate, all the other operating parameters remaining equal. It shows that at low particle flow rate, the outlet conversion rate is close to 100% because the residence time of the particles is high enough to complete the calcination reaction. As the flow rate is increased, the residence time of the particles in the reactor decreases as well as the conversion rate. In the meanwhile, the thermochemical efficiency of the process is increased because the higher the particle flow rate, the lower the equilibrium temperature of the reactor and hence the lower the heat losses to the outside. However, Fig. 6 shows that the chemical efficiency of the process reaches a maximum value (around 9% for 12.5 kg/h of particles). Below this optimal flow rate, one part of the heat provided to the reactor is not efficiently consumed by the calcination since the reaction extent is close to its maximum. Above the optimal flow rate, the decreasing equilibrium temperature hinders the reaction kinetics and reduces the conversion rate.

Figure 7 shows that the lower the fluidization flow rate, the higher is the conversion rate and hence the chemical efficiency. Even if a high fluidization flow rate improves the reaction kinetics by reducing the CO_2 concentration in the reactor, this phenomenon is compensated by the reduction of the fluidized bed porosity. Therefore, at low fluidization flow rate, the quantity of particles in the reactor, and therefore the mean residence time of the particles, is higher, which increases the conversion rate and the chemical efficiency. The thermochemical efficiency is weakly affected by the fluidization flow rate. It is slightly increased at high fluidization flow rate because the airflow cools down the reactor and hence reduces heat losses to the outside.

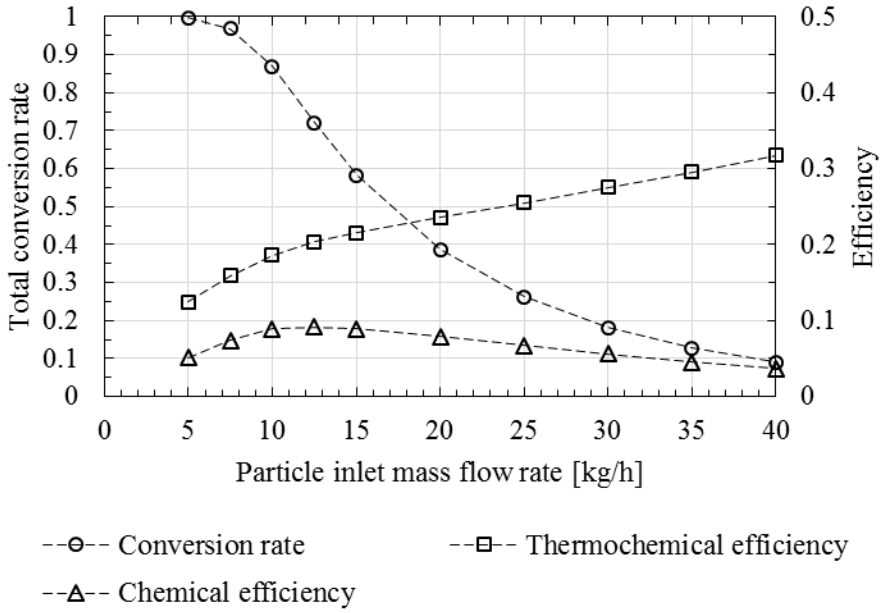

FIGURE 6. Influence of the inlet particle mass flow (F_{air} = 15 Nm^3/h)

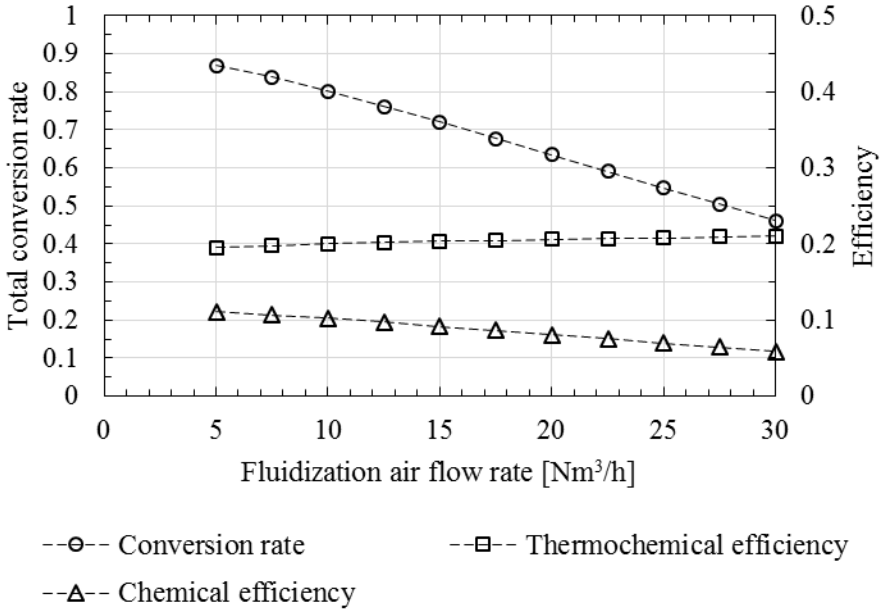

FIGURE 7. Influence of the fluidization air flow rate ($F_{p,in}$ = 12.5 kg/h)

Since the model has not been firmly validated yet, this parametric study only aims at showing the main trends of the reactor behaviour. The values of the performance parameters are only indicative and are still to be experimentally confirmed with the ongoing experiments. In particular, they are very sensitive to the reaction kinetics.

CONCLUSION

A pilot fluidized bed reactor for continuous calcination processes is tested at the CNRS's 1MW solar furnace. The first experimental results show that the reactor is able to perform the continuous thermal decomposition of calcite with

concentrated solar power. Around 20 kg/h of calcite were treated to produce lime with a conversion rate around 20%. An electrical air preheater and the refinement of the heliostat aiming strategy will be implemented to increase the performance of the reactor. In the meanwhile, a numerical model accounting for the energy and the mass balances of the calcination process has been developed. Further experimental data are necessary to validate the model. However, since it accounts for the main physical phenomena of the process, it can be used to study the pattern of behaviour of the system depending of the operating parameters. A parametric study showed that the outlet conversion rate is mainly governed by the mean residence time of the particles when a maximum solar-irradiated wall is imposed. Furthermore, there is an optimal particle flow rate that corresponds to a compromise between the reaction extent and the equilibrium temperature of the reactor, and which maximizes the chemical efficiency of the process.

ACKNOWLEDGMENTS

This project has received funding from the European Union's Horizon 2020 research and innovation programme under grant agreement No. 654663, SOLPART project. This work was supported by the French "Investments for the future", program managed by the National Agency for Research under contract "ANR-10-EQPX-49-SOCRATE" (Equipex SOCRATE).

REFERENCES

1. A. Imhof, "Calcination of limestone in a solar reactor", in *ZKG International*, 53(9), pp. 504–509, 2000.
2. V. Nikulshina, M. Halmann and A. Steinfeld, "Coproduction of Syngas and Lime by Combined CaCO3-Calcination and CH4-Reforming Using a Particle-Flow Reactor Driven by Concentrated Solar Radiation", *Energy & Fuels*, 23(12), pp. 6207–6212, 2009.
3. A. Steinfield, A. Imhof and D. Mischler, "Experimental Investigation of an Atmospheric-Open Cyclone Solar Reactor for Solid-Gas Thermochemical Reactions", *Journal of Solar Energy Engineering, Transactions of the ASME*, 114(3), pp. 171–174, 1991.
4. S. Abanades and L. André, "Design and demonstration of a high temperature solar-heated rotary tube reactor for continuous particles calcination", *Applied Energy*, 212, pp. 1310–1320, 2018.
5. G. Flamant, D. Hernandez, C. Bonet and J.-P. Traverse, "Experimental aspects of the thermochemical conversion of solar energy; Decarbonation of CaCO3", *Solar Energy*, 24(4), pp. 385–395, 1980.
6. A. Meier, E. Bonaldi, G.M. Cella, W. Lipinski and D. Wuillemin, "Solar chemical reactor technology for industrial production of lime", *Solar Power and Chemical Energy Systems (SolarPACES'04)*, 80(10), pp. 1355–1362, 2006.
7. G. Moumin, S. Tescari, P. Sundarraj, L. de Oliveira, M. Roeb, C. Sattler, "Solar treatment of cohesive particles in a directly irradiated rotary kiln", *Solar Energy*, 182, pp. 480–90, 2019.
8. C. Tregambi, P. Salatino, R. Solimene and F. Montagnaro, "An experimental characterization of Calcium Looping integrated with concentrated solar power", *Chemical Engineering Journal*, 331, pp. 794–802, 2018.
9. D. Geldart, "Types of gas fluidization", *Powder Technology*, 7(5), pp. 285–92, 1973.
10. O. Molerus, A. Burschka and S. Dietz, "Particle migration at solid surfaces and heat transfer in bubbling fluidized beds—II. Prediction of heat transfer in bubbling fluidized beds", *Chemical Engineering Science*, 50(5), pp. 879–885, 1995.
11. T.E. Broadhurst and H.A. Becke, "Onset of fluidization and slugging in beds of uniform particles", *AIChE Journal*, 21(2), pp. 238–247, 1975.
12. S. Wahl, "Nouvelle technologie de concentration de CO2 intégrée à la cimenterie : étude d'un nouveau procédé de décarbonatation", Ph.D. thesis, Université de Toulouse, 2018.
13. J.B. Rawlings and J.G. Ekerdt, *Chemical Reactor Analysis and Design Fundamentals* (Nob Hill Publishing, C.M. Rawlings, Madison, Wisconsin, 2002).
14. N.S. Grewal, "Experimental and theoretical investigations of heat transfer between a gas-solid fluidized bed and immersed tubes", Ph.D. thesis, Illinois University, 1979.